Electronic Materials: Science & Technology

Sean R. Bishop
Nicola H. Perry
Dario Marrocchelli
Brian W. Sheldon *Editors*

# Electro-Chemo-Mechanics of Solids

Springer

# Electronic Materials: Science & Technology

**Series editor**

Harry L. Tuller, Cambridge, MA, USA

The series *Electronic Materials: Science and Technology* will address the following goals:

- Bridge the gap between theory and application
- Foster and facilitate communication among materials scientists, electrical engineers, physicists and chemists
- Provide publication with an interdisciplinary approach in the following topic areas:

  - Sensors and Actuators
  - Electrically Active Ceramics and Polymers
  - Structure-Property-Processing-Performance Correlations in Electronic Materials
  - Electronically Active Interfaces
  - High Tc Superconducting Materials
  - Optoelectronic Materials
  - Composite Materials
  - Defect Engineering
  - Solid State Ionics
  - Electronic Materials in Energy Conversion
  - Solar Cells, High Energy Density Microbatteries, Solid State Fuel Cells, etc.

More information about this series at http://www.springer.com/series/5915

Sean R. Bishop · Nicola H. Perry
Dario Marrocchelli · Brian W. Sheldon
Editors

# Electro-Chemo-Mechanics of Solids

Springer

*Editors*
Sean R. Bishop
Massachusetts Institute of Technology
Cambridge, MA
USA

Dario Marrocchelli
Massachusetts Institute of Technology
Cambridge, MA
USA

Nicola H. Perry
WPI-I2CNER, Kyushu University
Fukuoka
Japan

Brian W. Sheldon
Brown University
Providence, RI
USA

and

Massachusetts Institute of Technology
Cambridge, MA
USA

ISSN 1386-3290
Electronic Materials: Science & Technology
ISBN 978-3-319-51405-5 ISBN 978-3-319-51407-9 (eBook)
DOI 10.1007/978-3-319-51407-9

Library of Congress Control Number: 2016960768



Printed on acid-free paper

This Springer imprint is published by Springer Nature
The registered company is Springer International Publishing AG
The registered company address is: Gewerbestrasse 11, 6330 Cham, Switzerland

# Preface

The purpose of this book is to introduce key advances in the study of electro-chemo-mechanics (ECM). ECM is the coupling between electrical, chemical, and mechanical properties and recently has received increasing attention. New experimental techniques and greater computational processing power have given us the ability to explore in greater detail how these materials properties are linked, as well as develop the models needed to apply ECM relationships in devices. Furthermore, as many individual materials reach maxima in their optimization through traditional means (e.g., through compositional control), additional variables, such as interfacing different materials together to, for example, achieve high states of strain, are opening new dimensions to materials property control. The chapters of this book cover ECM from both experimental and computational viewpoints, drawing on the increasing importance of linking the two research approaches. We hope that the chapters of this book, written by pre-eminent researchers in the field of ECM, increases both the reader's knowledge and enthusiasm for ECM. We acknowledge Prof. Harry Tuller at MIT for his suggestion and guidance in preparing this book.

Cambridge, MA, USA — Sean R. Bishop
Fukuoka, Japan — Nicola H. Perry
Cambridge, MA, USA — Dario Marrocchelli
Providence, RI, USA — Brian W. Sheldon

*The original version of the book was revised: For detailed information please see erratum. The erratum to this book is available at 10.1007/978-3-319-51407-9_8*

# Contents

# Chapter 1
# Introduction

**Sean R. Bishop and Nicola H. Perry**

Electro-chemo-mechanics is the relationship between electrical, chemical, and mechanical properties and the study of adjusting one property through the control of another (Fig. 1.1). This relationship can result in beneficial properties, for instance, mixed ionic and electronic conductivity in oxides upon oxygen deficiency or lithium insertion (electro-chemo) [1] and/or changes in ionic and electronic mobility observed in strained systems (electro-mechano) [2]. This relationship can also be responsible for detrimentally large stresses from non-stoichiometry-induced lattice dilation (chemo-mechano) [3]. While the origins and characteristics of the electro-chemical relationships have been the focus of many studies, much less is known about the corresponding electro-mechanical, chemo-mechanical, and electro-chemo-mechanical relationships. When designing new materials, one needs to be cognizant of the latter relationship. For example, deleterious chemical expansion was successfully decreased by decreasing the effective size oxygen vacancies have in the lattice [4], but at the expense of dramatically reduced ionic conductivity [5]. Optimizing the electro-chemo-mechanical response of new materials is aided by recent fundamental studies examining the role that factors such as cation radii size, relaxations in the lattice due to defect formation, and electronic and crystal structure play [6–11]. The purpose of this book is to present summaries

The author names "Dario Marrocchelli" and "Brian Sheldon" and their corresponding affiliations which were included earlier has been deleted now. The erratum to the book is available at 10.1007/978-3-319-51407-9

S.R. Bishop (✉) · N.H. Perry (✉)
Massachusetts Institute of Technology, Cambridge, MA, USA
e-mail: sean@redoxpowersystems.com

N.H. Perry
e-mail: perry@i2cner.kyushu-u.ac.jp

N.H. Perry
WPI-I2CNER, Kyushu University, Fukuoka, Japan



S.R. Bishop et al. (eds.), *Electro-Chemo-Mechanics of Solids*,
Electronic Materials: Science & Technology,
DOI 10.1007/978-3-319-51407-9_1

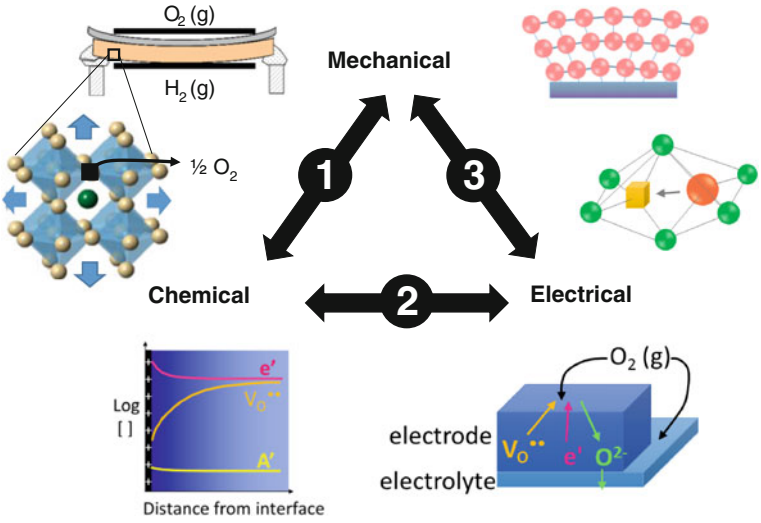


**Fig. 1.1** Overview of electro-chemo-mechanics: (*1*) chemo-mechanical coupling, e.g., chemically-induced stresses, (*2*) electro-chemical coupling, e.g., point-defect influenced transport and surface reaction kinetics, (*3*) mechano-electrical coupling, e.g., strain enhancements in carrier mobility

of some of the latest investigations in this coupling phenomenon, with applications to solid oxide fuel and electrolysis cells, as well as Li ion batteries. A summary of the book chapters is presented below.

The second chapter covers experimental methods that have been the workhorses of bulk ceramic studies. These methods include thermogravimetric analysis (TGA) and coulometric titration for examining oxygen content, and dilatometry to evaluate the corresponding defect induced expansion. Coupling these methods together over a wide range of oxygen partial pressure and temperature studies enables characterization of a key chemo-mechanical figure of merit, the chemical expansion coefficient, also known as the stoichiometric expansion coefficient [3]. Chapters 3 and 4 focus on the use of X-ray diffraction (XRD) and neutron diffraction (ND) experiments, respectively, to directly quantify chemical expansion of the crystal lattice. These techniques have the advantage of readily evaluating anisotropic expansion and, particularly for ND, determining atomic positions. Over the past few decades, these techniques have been improved to accommodate in situ measurements (i.e., elevated temperatures to greater than 1000 °C in controlled atmospheres). As thin films have increased in popularity due to the ability to constrain films with very large strains by controlling the substrate, techniques, such as XRD, have proven invaluable for their characterization. In Chap. 5, wafer curvature, an in situ method for examining the stress of thin films, is introduced. In addition to evaluating elastic properties of films, when coupled with XRD analysis, wafer curvature provides a noncontact method for evaluating the kinetics of oxygen uptake and release in thin films, a key electrochemical figure of merit for solid oxide

fuel cell applications. Chapter 6 moves to probing electro-chemo-mechanical coupling at the nanoscale by using in situ scanning probe microscopy (SPM) techniques. As microstructural features, such as grain boundaries and grains, are expected to play a key role in electro-chemo-mechanics, the high spatial resolution of SPM, coupled with electrochemical tools, enables direct evaluation of these features. The detailed knowledge of electro-chemo-mechanical response of materials provided by the above techniques would be of little use if it were not for predictive modeling of material behavior. In Chap. 7, continuum level modeling of transport and mechanics, making use of the above parameters, is presented. In this chapter, a clear visualization of the electro-chemo-mechanical effect is demonstrated.

This book presents only some of the recent activity in this field, and it is both the authors' and editors' desire to see continued growth in understanding electro-chemo-mechanical coupling phenomena.

## References


1. Tuller, H. L., & Bishop, S. R. (2011). Point defects in oxides: tailoring materials through defect engineering. *Annual Review of Materials Research, 41,* 369–398.
2. Mayeshiba, T., & Morgan, D. (2015). Strain effects on oxygen migration in perovskites. *Physical Chemistry Chemical Physics: PCCP, 17,* 2715–2721.
3. Bishop, S. R., et al. (2014). Chemical expansion: implications for electrochemical energy storage and conversion devices. *Annual Review of Materials Research, 44,* 205–239.
4. Bishop, S. R., et al. (2013). Reducing the chemical expansion coefficient in ceria by addition of zirconia. *Energy & Environmental Science, 6,* 1142–1146.
5. Ruehrup, V., & Wiemhoefer, H.-D. (2006). Ionic conductivity of Gd- and Y-doped ceria-zirconia solid solutions. *Zeitschrift für Naturforschung B [Journal of Chemical Sciences], 61,* 916–922.
6. Marrocchelli, D., Perry, N. H., & Bishop, S. R. (2015). Understanding chemical expansion in perovskite-structured oxides. *Physical Chemistry Chemical Physics: PCCP, 17,* 10028–10039.
7. Perry, N. H., Bishop, S. R., & Tuller, H. L. (2014). Tailoring chemical expansion by controlling charge localization: In situ X-ray diffraction and dilatometric study of (La, Sr)(Ga, Ni)$O_{3-\delta}$ perovskite. *Journal of Materials Chemistry A, 2,* 18906–18916.
8. Marrocchelli, D., Bishop, S. R., Tuller, H. L., Watson, G. W., & Yildiz, B. (2012). Charge localization increases chemical expansion in cerium-based oxides. *Physical Chemistry Chemical Physics: PCCP, 14,* 12070–12074.
9. Marrocchelli, D., Bishop, S. R., Tuller, H. L., & Yildiz, B. (2012). Understanding chemical expansion in non-stoichiometric oxides: Ceria and zirconia case studies. *Advanced Functional Materials, 22,* 1958–1965.
10. Perry, N. H., Kim, J. J., Bishop, S. R., & Tuller, H. L. (2015). Strongly coupled thermal and chemical expansion in the perovskite oxide system Sr(Ti, Fe)$O_{3-\alpha}$. *Journal of Materials Chemistry A, 3,* 3602–3611.
11. Perry, N. H., Marrocchelli, D., Bishop, S. R., & Tuller, H. L. (2016). Understanding and controlling chemo-mechanical coupling in perovskite oxides. *Electrochemical Society*.

# Chapter 2
# Conventional Methods for Measurements of Chemo-Mechanical Coupling

**Andrey Yu. Zuev and Dmitry S. Tsvetkov**

Energy-related oxide materials are often used at elevated temperatures under both oxidizing and reducing conditions and, therefore, their chemical composition with respect to oxygen may change. Due to release of lattice oxygen and simultaneous point defect formation, their lattice can undergo additional defect-induced or, in other words, chemical strain, which, in turn, affects mechanical compatibility of different components of an energy conversion device, and can cause even its damage. Thus elucidation of chemo-mechanical coupling in such materials is of key importance. In order to solve this important task, oxygen content of oxide materials and their chemical strain should be measured depending on environmental parameters. The description of the state-of the-art methods for measuring oxygen content, such as thermogravimetry, coulometric and redox titration, as well as some examples of their employment, are given in this chapter. Dilatometry, as a conventional method for strain measurement, is described as well. Also this chapter is intended to show how insight into mechano-chemical coupling mechanisms can be established on the basis of the aforementioned measurements.

A.Yu. Zuev (✉) · D.S. Tsvetkov
Department of Chemistry, Institute of Natural Sciences, Ural Federal University, Yekaterinburg 620000, Russia
e-mail: andrey.zuev@urfu.ru

D.S. Tsvetkov
e-mail: dmitry.tsvetkov@urfu.ru



S.R. Bishop et al. (eds.), *Electro-Chemo-Mechanics of Solids*,
Electronic Materials: Science & Technology,
DOI 10.1007/978-3-319-51407-9_2

## 2.1 Methods for Measuring Oxygen Content and Analysis of the Defect Structure of Oxide Materials

### *2.1.1 TG Analysis (with Examples)*

Thermogravimetry (TG) is a thermal analysis method based on detection of sample mass change depending on temperature and other parameters (e.g., gas phase composition—oxides are usually studied depending on partial pressure of oxygen, $pO_2$). There are two ways to employ TG analysis: (i) isothermal—at constant temperature, and (ii) isobaric—when temperature is changed with time at constant gas (partial) pressure. Thermogravimetric analysis can be used to measure oxygen nonstoichiometry of oxides with low volatility and a wide homogeneity range with respect to oxygen. The former requirement is necessary because high volatility of cation species in an oxide can contribute to its irreversible mass change. The setup for TG consists of a balance for continuous weighing, furnace, instrument recording temperature, temperature controller, and software. Figure 2.1 shows a sketch of the thermobalance STA 409 PC (Netzsch Gmbh, Germany), which is often used for TG analysis.

Different oxygen partial pressures are adjusted and maintained in the vicinity of the sample by using different gas mixtures (for example, $N_2/O_2$ or $H_2/N_2$). The composition of the corresponding gas mixture is controlled using precise flow controllers and the value of $pO_2$ is fixed by means of an yttria stabilized zirconia (YSZ) electrochemical oxygen sensor installed in close proximity to the sample surface in the TG setup (see Fig. 2.1). Alternatively the concentration of oxygen in the gas atmosphere around the sample can be adjusted using a YSZ-based electrochemical oxygen pump installed in the outer regulating unit and governed by an automatic controller. Adjusted accordingly, $pO_2$ is monitored by means of an installed YSZ sensor giving feedback to the control system (see Fig. 2.1). The latter method of control is more precise and flexible as well as it makes using of expensive gas cylinders unnecessary. Typically, a gas flow rate of about 30–50 ml/min is used to avoid oxygen partial pressure gradients along the sample.

The sample of studied oxide is heated first to the required temperature in an atmosphere with a given $pO_2$ (most often ambient air), then is equilibrated at this $pO_2$ and temperature for the necessary time until the sample weight ceases to change. Then measurements are carried out either in an isothermal or isobaric regime. In the case of the former, oxygen partial pressure is changed in steps within the range between initial and final values of $pO_2$ in both decreasing and increasing directions at the same temperature, and the measurement procedure is repeated until the equilibrium state is reached at each step, i.e., until weight curves recorded in both directions coincide with each other. In the isobaric regime, temperature is changed in steps within the range between initial and final values at the same $pO_2$, and the rest of the experimental procedure is similar to that described for isothermal regime.

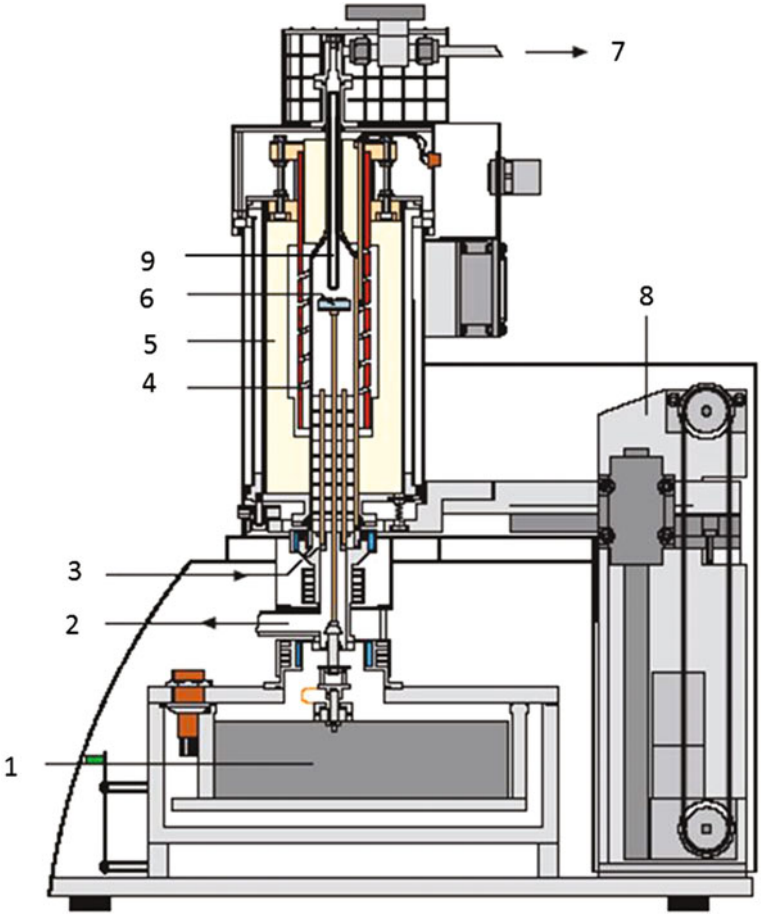


**Fig. 2.1** TG setup based on thermobalance STA 409 PC: *1* weight unit, *2* vacuum flange, *3* gas inlet, *4* $Al_2O_3$ vacuum-tight protective tube, *5* furnace, *6* crucible with a sample studied, *7* gas outlet, *8* hoist, *9* YSZ sensor. Earlier available at https://www.netzsch-thermalanalysis.com

Oxygen exchange between an oxide, for example, perovskite $ABO_{3-\delta}$, and ambient gas atmosphere can be written as

$$ABO_{3-\delta} \Leftrightarrow ABO_{3-\delta-\Delta\delta} + \frac{\Delta\delta}{2}O_2 \tag{2.1}$$

where $\Delta\delta$ is a change in the oxygen content or, in other words, relative oxygen nonstoichiometry of the oxide, which can be calculated from the weight change by the following expression.

$$\Delta\delta = \frac{\Delta m_{\text{sample}}}{m_{0,\text{sample}}} \cdot \frac{M^0_{\text{ABO}_{3-\delta}}}{M_{\text{O}}} \tag{2.2}$$

where $m_{0,\text{sample}}$, $\Delta m_{\text{sample}}$, $M^0_{\text{ABO}_{3-\delta}}$, $M_{\text{O}}$ are starting weight of the $\text{ABO}_{3-\delta}$ sample, its weight change caused by temperature or $p\text{O}_2$ variation, starting molar weight of the sample, and molar weight of oxygen (15.9994 g/mol), respectively.

In order to recalculate relative oxygen nonstoichiometry ($\Delta\delta$) on an absolute scale ($\delta_{\text{total}}$), it is necessary to determine the absolute oxygen content in the oxide studied at some particular value of $p\text{O}_2$ and temperature lying within the range investigated. This can be implemented by means of either sample reduction by $\text{H}_2$ in a thermobalance (TG/$\text{H}_2$) or sample redox titration. Both methods will be described further.

### 2.1.2 Coulometric Titration in Solid State Electrolyte Cell (with Examples)

Coulometric titration is the most precise method for determination of the oxygen content change in solid-oxide phases. This method can be employed to study oxides with both wide and narrow homogeneity ranges with respect to oxygen and with both high and low volatility. The method is based on using the electrochemical concentration cell (2.3) with an oxide ion conducting solid electrolyte (typically YSZ) and with gas electrodes operating at different oxygen partial pressure ($p\text{O}_2$) and separated from each other

$$\text{Pt}, p\text{O}_2'', \text{MeO}_x|\text{ZrO}_2(\text{Y}_2\text{O}_3)|p\text{O}_2', \text{Pt} \tag{2.3}$$

where $\text{MeO}_x$ is an oxide under investigation, $p\text{O}_2'$ and $p\text{O}_2''$ are oxygen partial pressure in the gas equilibrated with the oxide studied and that at the reference electrode, respectively. A schematic of the cell is shown in Fig. 2.2.

The EMF of the cell (2.3) is related to $p\text{O}_2'$ and $p\text{O}_2''$ by the Nernst equation, written below.

$$E = \frac{RT}{4F} \cdot \ln\left(\frac{p\text{O}_2''}{p\text{O}_2'}\right) \tag{2.4}$$

where $F$, $T$, $p\text{O}_2''$, $p\text{O}_2'$, 4, and $R$ are Faraday constant (s A/mol), temperature (K), oxygen partial pressure inside the cell (Pa), oxygen partial pressure outside the cell, number of electrons taking part in the electrode reaction, and universal gas constant (J/(mol K)), respectively.

A DC current is periodically applied to the titration cell (2.3) and, as a consequence, oxygen is pumped in or out of the gas phase surrounding the oxide studied depending on polarization or, in other words, current direction by an equal

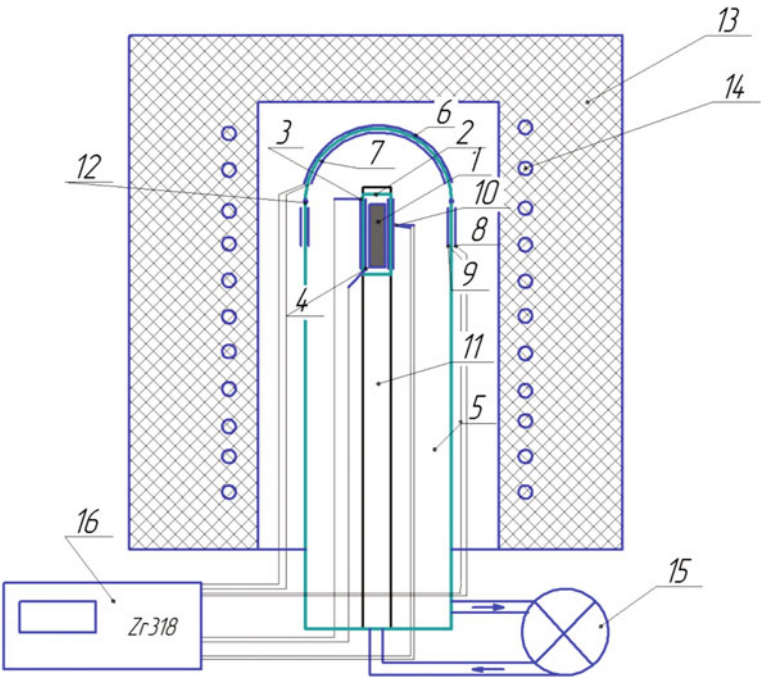


**Fig. 2.2** Setup for coulometric titration: *1* sample studied; *2* YSZ coulometric cell; *3*, *4* Pt electrodes of coulometric cell; *5* YSZ buffer cell; *6*, *7* Pt electrodes of electrochemical pump of the buffer cell; *8*, *9* Pt electrodes of electrochemical sensor of the buffer cell; *10* Pt/Rh thermocouple; *11* alumina cell holder; *12* sealing glass; *13* furnace; *14* heater; *15* gas circulation pump; *16* managing controller. Ref. [3]

proportion. Each titration step is followed by the relaxation of the sample to the equilibrium state coinciding with a new oxygen partial pressure at given temperature. The oxygen nonstoichiometry change is calculated at each titration step according to

$$\Delta\delta = \frac{2M}{m}\left[\frac{It}{4F} - \frac{V}{RT}\left(p\mathrm{O}_2''(b) - p\mathrm{O}_2''(a)\right)\right] \tag{2.5}$$

where $M$, $m$, $I$, $t$, $V$, $p\mathrm{O}_2''(b)$, $p\mathrm{O}_2''(a)$ are oxide investigated molar mass (g/mol), oxide sample mass (g), titration current (A), titration time (s), free volume of the coulometric cell ($m^3$), oxygen partial pressure before titration step (Pa), oxygen partial pressure after titration step (Pa), respectively.

In principle, a coulometric cell can be easily assembled using a dense YSZ ceramic tube closed at one side with previously deposited Pt contacts on inner and outer sides. In this case, the oxide sample is put in the inner part of the tube, which serves as a working electrode operating at $p\mathrm{O}_2''$, and its outer side serves as a reference electrode operating at $p\mathrm{O}_2'$. However, a serious disadvantage of this cell

design is the so-called non-faradaic leakage of oxygen into/out of the coulometric cell due to nonnegligible electronic conduction in YSZ.

In order to prevent undesirable leakage the cell supplied by gas buffer can be used. Such a coulometric setup is shown in Fig. 2.2.

As seen the coulometric setup consists of two YSZ cells: an external one (5), which is used as a buffer, and an internal one (2), which is a coulometric cell itself. Both cells serve simultaneously as an oxygen pump (3, 4, 6, 7) and as a sensor (3, 4, 8, 9) due to platinum contacts deposited on both the inner and outer surfaces of a cell. The coulometric cell is hermetically sealed using special glass and contains a sample of the oxide investigated (1). The buffer cell (5) is used to control oxygen partial pressure around the coulometric cell using the oxygen pump (6, 7) and sensor (8, 9) in such way that a value of $pO_2$ outside the coulometric cell is always kept about equal to that inside it. Such design of the setup allows avoiding even very small non-faradaic leakage of oxygen into/out of the coulometric cell. In order to measure $pO_2$ around the sample inside the coulometric cell its oxygen sensor and that of the buffer cell are connected in series. Titration current is periodically applied to the titration cell and, as a consequence, oxygen is pumped in or out of the cell by equal portions. Each titration step is followed by the relaxation of the sample to a new equilibrium state at a new oxygen partial pressure at given temperature. The coulometric titration procedure can be fully automatized using a managing controller (16) connected to computer. Such a system enables control and adjustment of oxygen partial pressure within the range $-20 \le \log(pO_2/\text{atm}) \le 0$ with accuracy $\pm 0.01$ in the immediate vicinity of the coulometric cell. Gas circulation (15) is used to avoid an oxygen partial pressure gradient along the titration cell. The oxygen nonstoichiometry change is calculated at each titration step according to Eq. (2.5).

Since Eq. (2.5) enables calculation of only the relative change of the oxygen nonstoichiometry, to get its absolute value, similar to TG analysis, an additional experiment such as $H_2$ reduction in a thermobalance or redox titration is needed.

It is worth noting general limitation on applicability of coulometric titration using YSZ-based cell at relatively low temperatures due to the large overpotentials at the Pt electrodes and insufficient conductivity of YSZ, making low temperature measurements difficult.

### 2.1.3 *Determination of the Absolute Value of Oxygen Nonstoichiometry*

As mentioned above, both TG and coulometric titration enable measurement of only the relative change of oxygen nonstoichiometry, $\Delta\delta$, in oxide compounds. The absolute value of $\delta$ can be measured using several methods, for instance, reduction of an oxide sample by hydrogen flux directly in the TG setup or chemical analysis of the sample previously quenched or slowly cooled from certain conditions

($T$, $pO_2$). However, there is another way for the oxide compounds, which have a plateau on the $pO_2$ dependency of relative oxygen nonstoichiometry plotted at a given temperature. In such cases, this plateau corresponds to a certain, and as a rule, known value of the oxygen content in the oxide studied. For instance, lanthanum manganite $LaMnO_{3\pm\delta}$ has both excess ($3 + \delta$) and deficiency region ($3 - \delta$) with respect to oxygen content depending on temperature and $pO_2$ and its absolute oxygen nonstoichiometry is exactly equal to zero when the plateau between these regions is reached during coulometric titration or TG procedure (see Fig. 2.5).

#### 2.1.3.1 Direct Reduction of Oxide Sample by Hydrogen

A sample of the oxide studied is heated in a thermobalance chamber to the required temperature in atmosphere with a given $pO_2$ (most often ambient air) and then is equilibrated at this $pO_2$ and temperature for the necessary time until the sample weight ceases to change. Afterwards hydrogen flow is passed through the chamber previously purged with an inert gas until the weight of the sample becomes unchangeable. The value of this weight is used for calculation of absolute oxygen nonstoichiometry of the oxide compound according to the products of its reduction. Products of the reduction are determined by XRD of the sample cooled down fast after the completion of the reduction procedure. For example, if the sample of a perovskite $ABO_{3-\delta}$ is reduced in hydrogen flux according to the following reaction

$$ABO_{3-\delta} + \left(\frac{3}{2} - \delta\right)H_2 = \frac{1}{2}A_2O_3 + B + \left(\frac{3}{2} - \delta\right)H_2O \tag{2.6}$$

then the oxygen nonstoichiometry $\delta$ can be calculated as

$$\delta = \frac{m_{red} \cdot M_{st} - m_{ox} \cdot \left(\frac{M_{A_2O_3}}{2} + M_B\right)}{m_{red} \cdot M_O} \tag{2.7}$$

where $m_{red}$, $m_{ox}$, $M_{st}$, $M_{A_2O_3}$, $M_B$, and $M_O$ are weight of the reduced and oxidized (before reduction) sample, molar weight of the $ABO_3$ stoichiometric with respect to oxygen, molar weight of oxide $A_2O_3$, metal B, and elemental oxygen, respectively.

#### 2.1.3.2 Iodometric Determination of the Absolute Oxygen Nonstoichiometry

Iodometric method is based on Ox–Red processes related to reduction of iodine into iodide ions or in oxidation of iodide ions into molecular iodine. Normally the sample is dissolved in an acidic solution containing an excess of iodide ions. Molecular iodine obtained as a result of interaction between the oxidant and iodide ions is titrated with standard sodium thiosulfate solution. Both oxide dissolution

and successive titration should be carried out under an inert gas protective atmosphere to prevent iodide oxidation by oxygen from the air. Now let us consider the following example. Suppose we have a B cation in a perovskite $ABO_{3-\delta}$ in a mixed state of oxidation $n+$, and during dissolution and simultaneous interaction with iodide ions it reduces to $B^{2+}$ while the A cation and oxygen do not change their oxidation states, then the following reactions can be written

$$2B^{n+} + 2(n-2)J^- \rightarrow 2B^{2+} + (n-2)J_2 \tag{2.8}$$

$$\frac{1}{2}I_2 + e' \rightarrow I^- \tag{2.9}$$

$$2S_2O_3^{2-} - 2e' \rightarrow S_4O_6^{2-} \tag{2.10}$$

Since the thiosulfate volume spent for iodine titration is known, the mean state of oxidation $n+$ of B cation in the perovskite $ABO_{3-\delta}$ can be calculated using the obvious relation

$$n = \frac{(CV)_{S_2O_3^{2-}}}{v} + 2, \tag{2.11}$$

where $v$, $C_{S_2O_3^{2-}}$, $V_{S_2O_3^{2-}}$ are number of moles of B cation, molarity, and volume of thiosulfate solution used, respectively.

The absolute oxygen nonstoichiometry in the perovskite $A^{z+}B^{n+}O_{3-\delta}^{2-}$ studied is calculated on the basis of electroneutrality condition as

$$\delta = 3 - \frac{z+n}{2}. \tag{2.12}$$

### 2.1.4 Some Examples of the Study of Oxygen Nonstoichiometry by TG and Coulometric Titration Methods

Typical results of TG analysis demonstrating sample weight change caused by temperature variation at a given $pO_2$ or $pO_2$ variation at a given temperature are shown in Fig. 2.3.

Taking into account weight changes of the sample $GdBaCo_2O_{6-\delta}$ obtained in an analogous way for different $pO_2$ within the range investigated, the relative change of the oxygen nonstoichiometry can be calculated according to the relation analogous to Eq. (2.2) and then recalculated on an absolute scale on the basis of the results of TG/$H_2$ reduction or/and Ox–Red titration. As a result, the oxygen nonstoichiometry ($\delta$) of the double perovskite $GdBaCo_2O_{6-\delta}$ measured [1] as a function of $pO_2$ and temperature in the ranges $-6 \le \log(pO_2/\text{atm}) \le -0.68$ and

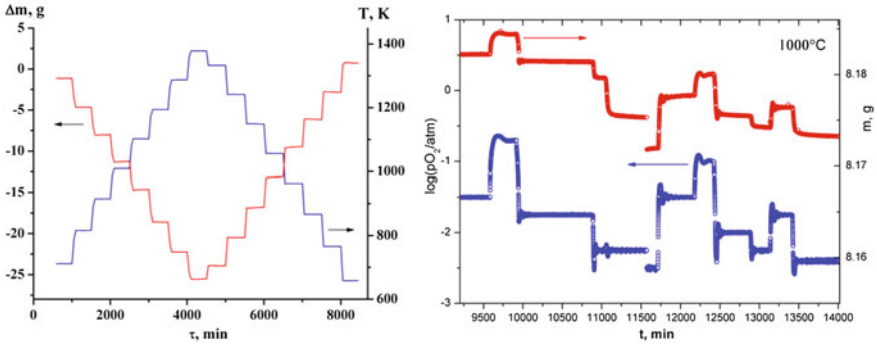


**Fig. 2.3** Raw trace of sample weight for $GdBaCo_2O_{6-\delta}$ as a function of temperature in air (*left*) and $La_{0.8}Sr_{0.2}Co_{0.9}Ni_{0.1}O_{3-\delta}$ as a function of $pO_2$ at 1000 °C (*right*)

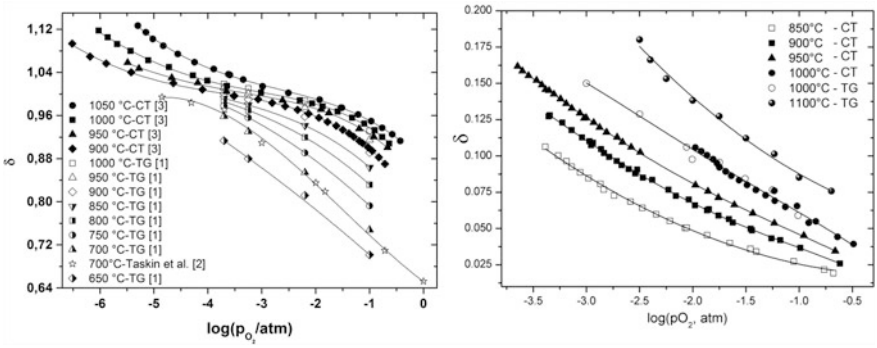


**Fig. 2.4** Oxygen nonstoichiometry of $GdBaCo_2O_{6-\delta}$ (*left*) [1] and $La_{0.8}Sr_{0.2}Co_{0.9}Ni_{0.1}O_{3-\delta}$ (*right*) [17] as a function of $pO_2$ at different temperatures. *Points* are experimental data and *lines* are given for eye guide. *CT* coulometric titration, *TG* thermogravimetry

$923 \leq T, K \leq 1323$, respectively, is given in Fig. 2.4 in comparison with the data reported by Taskin et al. [2]. As seen there is good agreement between the values of oxygen nonstoichiometry obtained by TG [1] and those measured by Taskin et al. [2]. It also follows from Fig. 2.4 that oxygen nonstoichiometry determined by means of the coulometric titration technique [3] and one measured by the TG method [1] are completely coincident with each other.

Another example of successful joint employment of TG and coulometric techniques is shown in Fig. 2.4 where oxygen nonstoichiometry of the perovskite $La_{0.8}Sr_{0.2}Co_{0.9}Ni_{0.1}O_{3-\delta}$ is given as a function of $pO_2$ and temperature as well. As seen in the figure, the oxygen nonstoichiometry values determined by both techniques are completely coincident with each other, as likewise demonstrated for those for $GdBaCo_2O_{6-\delta}$ discussed above.